Hybrid matter-wave - microwave solitons on the lattice

Zhihuan Luo[1], Weiwen Luo[1], Wei Pang[2], Zhijie Mai[1], Yongyao Li[3]* and Boris A. Malomed[4,1]†

[1] *Department of Applied Physics, South China Agricultural University, Guangzhou 510642, China*
[2] *Department of Experiment Teaching, Guangdong University of Technology, Guangzhou 510006, China*
[3] *School of Physics and Optoelectronic Engineering, Foshan University, Foshan 528000, China*
[4] *Department of Physical Electronics, School of Electrical Engineering, Faculty of Engineering,*
and the Center for Light-Matter Interaction, Tel Aviv University, Tel Aviv 69978, Israel

We introduce a two-component system which models a pseudospinor Bose-Einstein condensate (BEC), with a microwave field coupling its two components. The feedback of BEC of the field (the local-field effect) is taken into account by dint of the respective Poisson equation, which is solved using the Green's function. This gives rise to an effective long-range self-trapping interaction, which may act alone, or be combined with the contact cubic nonlinearity. The system is made discrete by loading the BEC into a deep optical-lattice potential. Numerical solutions demonstrate that onsite-centered fundamental solitons are stable in the cases of attractive or zero contact interactions, while offsite-centered solitons are unstable. In the case of the repulsive onsite nonlinearity, offsite solitons are stable, while their onsite-centered counterparts are stable only at sufficiently small values of the norm, where bistability between the off- and onsite-centered mode takes place. The shape of the onsite-centered solitons is very accurately predicted by a variational approximation (which includes essential technical novelties). Spatially-antisymmetric ("twisted") solitons are stable at small values of the norm, being unstable at larger norms. In the strongly asymmetric version of the two-component system, which includes the Zeeman splitting, the system is reduced to a single discrete Gross-Pitaevskii equation, by eliminating the small higher-energy component.

I. INTRODUCTION

It is well known that a pair of couterpropagating coherent optical waves produce an effective dipole potential for cold atoms, in the form of an optical lattice (OL). OL-induced potentials play a well-known role in dynamics of quantum atomic gases, helping to create gap solitons and other species of collective modes [1, 2]. The feedback of the atomic motion on the light propagations, alias the local-field effect (LFE), produces a deformation of the OL. The LFE is often weak, due to the far detuning of the OL's frequency from the atomic resonance. Nevertheless, in some situations, such as the diffraction of Bose-Einstein condensates (BECs) on optical waves with unequal intensities [3], LFE is a significant factor. In particular, it can make the underlying OL relatively "soft", inducing an effective nonlocal interaction [4], which, in turn, can create matter-wave solitons, even in the absence of contact interactions in the BEC [5].

Another manifestation of the LFE is a nonlinear correction to the coupling of two components of the wave function of a pseudospinor BEC, corresponding to two different hyperfine atomic states, via the magnetic component of the microwave (MW) field which resonantly couples these states [6, 7] (this is the difference from earlier studied cases, in which the electric component played a dominant role in the action of the LFE). The LFE-induced nonlinear correction is nonlocal in this case, as the magnetic field obeys the respective Poisson equation. The final result is a system of two Gross-Pitaevskii equations (GPEs) coupled by an effective nonlinear interaction, which is locally repulsive but globally attractive, thus opening a new way to create self-trapped hybrid matter-wave - microwave solitons.

It is well known that BECs, split into a chain of droplets by a deep OL potential, are adequately modeled, in the framework of the tightly-binding approximation for the droplets, by discrete GPEs. In this approximation, hopping between adjacent sites of the underlying lattice is represented by linear couplings between them [8]-[12]. If atoms in BEC carry permanent magnetic moments, the respective discrete GPE features long-range interactions between remote sites [13, 14], which, in particular, gives rise to stable on- and off-site centered solitons and periodically modulated extended patterns. In a more general context, discrete GPEs belong to the broad class of discrete nonlinear Schrödinger equations (NLSEs), which appear in a great variety of physical realizations [15, 16]. In this context, nonlocal interactions are also a topic of considerable interest [17].

The objective of the present work is to introduce a discrete version of the coupled GPE system with the strongly

---

*Electronic address: yongyaoli@gmail.com
†Electronic address: malomed@post.tau.ac.il

nonlocal nonlinearity, which was introduced in the continuum form in work [6]. It implies that the two-component BEC, resonantly coupled by the microwave field, is loaded in a deep OL potential, that leads to the effective discretization of the system. In addition to the physical significance of the model, it provides a novel variety of discrete NLSEs, with a specific long-range inter-site interaction. The system gives rise to specific on- and offsite-centered fundamental spatially even discrete solitons, as well as *twisted* [15, 18, 19] (spatially antisymmetric) ones. These soliton families are also quite different from those in the original continuum system, that were reported in work [6]. In particular, the width of the discrete fundamental solitons may be much smaller in comparison with their counterparts in the continuum limit.

The rest of the paper is organized as follows. The model is introduced in section II, which is followed by the presentation of numerical and analytical findings in sections II and III, respectively. In particular, analytical results for the fundamental on-site-centered solitons are obtained by means of a variational approximation (VA), which very accurately match the numerical findings, this version of the VA for discrete solitons being an essential technical novelty by itself. Further, the system with asymmetry between its components, induced by detuning (Zeeman splitting) between them, is studied in section IV. The paper is concluded by section V.

II.   THE MODEL

We consider the one-dimensional hybrid system introduced in [6]. It includes the pseudospinor (two-component) BEC, with wave functions of two hyperfine states coupled by the magnetic component of the microwave field. The feedback of the pseudospinor wave function on the microwave field, represented by the Poisson equation for the field, coupled to the system of two GPEs, which include the field, is a manifestation of the LFE in the present setting. The system is made discrete by fragmentation in a deep OL potential. As a result, the microwave field can be eliminated, solving the one-dimensional Poisson equation by means of the Green's function (similarly to how it was done in [6]). As a result, the system is modeled by coupled discrete GPEs for amplitudes (Ψ_n, Φ_n) of the pseudospinor wave function at OL sites, with discrete coordinate n:

$$i\frac{\partial \Psi_n}{\partial t} = -\frac{1}{2}\left(\Psi_{n+1} - 2\Psi_n + \Psi_{n-1}\right) + \eta\Psi_n - H_0\Phi_n + \gamma\Phi_n \sum_m |m-n| \Phi_m^* \Psi_m + \left(G\left|\Psi_n\right|^2 + \Gamma\left|\Phi_n\right|^2\right)\Psi_n,$$

$$i\frac{\partial \Phi_n}{\partial t} = -\frac{1}{2}\left(\Phi_{n+1} - 2\Phi_n + \Phi_{n-1}\right) - \eta\Phi_n - H_0\Psi_n + \gamma\Psi_n \sum_m |m-n| \Psi_m^* \Phi_m + \left(G\left|\Phi_n\right|^2 + \Gamma\left|\Psi_n\right|^2\right)\Phi_n. \quad (1)$$

In the general case, the system includes the self- and cross- contact interactions with coefficients G and Γ, respectively (alias the onsite nonlinearity, in terms of the lattice dynamics). The onsite interactions are repulsive, in the case of $G, \Gamma > 0$, and attractive, for $G, \Gamma < 0$. Further, the coefficient of the intersite hopping is scaled to be 1 in Eq. (1), η (which may be zero) is the strength of the Zeeman-splitting effect [20], which induces the detuning of two-component system, H_0 is the background magnetic field of the microwave, which induces linear mixing between the two components. The terms $\sim \gamma$ represent the long-range interaction generated by the magnetic field, the particular form of the interaction kernel in Eq. (1) being produced by the above-mentioned Green's function used for the solution of the one-dimensional Poisson equation.

Stationary states are looked for in the usual form,

$$(\Psi_n(t), \Phi_n(t)) = (\psi_n, \phi_n)e^{-i\mu t}, \quad (2)$$

where (ψ_n, ϕ_n) are stationary wave functions, and μ is a real chemical potential. The norms of the two components are defined as

$$N_\psi = \sum_n |\psi_n|^2, N_\phi = \sum_n |\phi_n|^2. \quad (3)$$

The relative norm difference between ψ_n and ϕ_n, which is induced by the Zeeman splitting, when it is present, is

$$\Delta = \frac{|N_\psi - N_\phi|}{N}. \quad (4)$$

Widths of the two components of the discrete soliton are defined as

$$W_\psi = \frac{\left(\sum_n |\psi_n|^2\right)^2}{\sum_n |\psi_n|^4}, W_\phi = \frac{\left(\sum_n |\phi_n|^2\right)^2}{\sum_n |\phi_n|^4}. \quad (5)$$

First, it is relevant to produce the dispersion relation for the linearized version of Eq. (1), substituting the solution in the form of $(\Psi_n(t), \Phi_n(t)) \sim \exp(-i\mu t + iqn)$ with real wavenumber q:

$$\mu = 2\sin^2(q/2) \pm H_0. \tag{6}$$

However, unlike models with the local nonlinearity, where bright solitons may be found solely in bandgaps of the spectrum, i.e., in intervals of the chemical potential which cannot be covered by values given by Eq. (6) with arbitrary real values of q, this commonly known principle does not apply to the present system, because the nonlocal nonlinear term in Eq. (1) grows $\sim |n|$ at $|n| \to \infty$, making the system *nonlinearizable*, as concerns the identification of the asymptotic shape of the soliton's shapes, i.e., necessary conditions admitting the existence of localized modes [6] (see also works [21, 22], as concerns more general classical and quantum discrete systems which admit bright solitons in nonlinearizable models with the repulsive nonlinearity).

III. THE SYMMETRIC SYSTEM (NO ZEEMAN SPLITTING)

A. The formulation

The long-range interaction in the hybrid system plays a crucial role in the creation of solitons. To reveal its nature, we first consider the basic case of zero-detuning, with $\eta = 0$ in Eq. (1). In this case, the equation for symmetric states, with $\Phi_n = \Psi_n$, reduces to

$$i\frac{\partial \Psi_n}{\partial t} = -\frac{1}{2}(\Psi_{n+1} - 2\Psi_n + \Psi_{n-1}) - H_0\Psi_n + \gamma\Psi_n\sum_m |m-n||\Psi_m|^2 + (G+\Gamma)|\Psi_n|^2\Psi_n. \tag{7}$$

By means of an obvious transformation,

$$\Psi_n(t) = \gamma^{-1/2}e^{iH_0 t}U_n(t), \tag{8}$$

one may cast Eq. (7) in the form of

$$i\frac{\partial U_n}{\partial t} = -\frac{1}{2}(U_{n+1} - 2U_n + U_{n-1}) + U_n\sum_m |m-n||U_m|^2 + g|U_n|^2 U_n, \tag{9}$$

which contains the single free parameter, $g \equiv (G+\Gamma)/\gamma$.

Then, stationary solutions with real chemical potential are looked for as

$$U_n(t) = e^{-i\mu t}u_n, \tag{10}$$

where discrete field u_n satisfies the equation

$$\mu u_n + \frac{1}{2}(u_{n+1} - 2u_n + u_{n-1}) = u_n\sum_m |m-n|u_m^2 + gu_n^3. \tag{11}$$

B. The variational approximation (VA)

The usual approach to constructing discrete solitons in nonlinear lattice models starts from the anti-continuum limit, which neglects the hopping between adjacent sites [16, 37] (in the continuum counterpart of the lattice model, it corresponds to the Thomas-Fermi approximation [38]). However, the application of the anti-continuum limit to Eq. (11) does not make the remaining equation solvable, because it includes the nonlocal interaction.

A more promising analytical approach may be based on the VA. To this end, we note that Eq. (11) can be derived from the Lagrangian,

$$L = -\frac{\mu}{2}N + H, \tag{12}$$

where the respective norm and Hamiltonian are

$$N = \sum_{n=-\infty}^{+\infty} u_n^2, \tag{13}$$

$$H = \frac{1}{4}\left\{\sum_{n=-\infty}^{+\infty}\left[(u_{n+1} - u_n)^2 + gu_n^4\right] + \sum_{m,n=-\infty}^{+\infty} |m-n|u_m^2 u_n^2\right\}. \tag{14}$$

Following the pattern of works [39]-[41], the variational ansatz for fundamental onsite-centered discrete solitons, with amplitude A and inverse width a, can be adopted as

$$u_n = A \exp\left(-a|n|\right). \tag{15}$$

Norm (13) of the ansatz is

$$N = A^2 \coth a. \tag{16}$$

The application of the VA to Lagrangian (12)-(14), which includes the long-range interaction, is a novel technical problem. Its solution is facilitated by the use of the following formulas, which appear in the course of the substitution of ansatz (15) in Lagrangian (12):

$$\sum_{n=-\infty}^{+\infty} e^{-2a|n|} = \coth a, \quad \sum_{n=-\infty}^{+\infty} \left(e^{-a|n+1|} - e^{-a|n|}\right)^2 = 2\tanh\left(\frac{a}{2}\right), \tag{17}$$

$$\sum_{m,n=-\infty}^{+\infty} |m-n| \, e^{-2a(|m|+|n|)} \equiv 2 \sum_{m \geq n=-\infty}^{+\infty} (m-n)\, e^{-2a(|m|+|n|)} = \frac{2\cosh(2a)+1}{2\sinh(2a)\cdot\sinh^2 a}. \tag{18}$$

Then, the effective Lagrangian corresponding to ansatz (15) is explicitly calculated as

$$
L_{\text{eff}} = -\frac{\mu}{2} A^2 \coth a + \frac{A^2}{2}\tanh\left(\frac{a}{2}\right) + \frac{gA^4}{4}\coth(2a)
$$
$$
+ \frac{A^4}{8}\frac{2\cosh(2a)+1}{\sinh(2a)\cdot\sinh^2 a} \ . \tag{19}
$$

Finally, the variational equations are derived from the Lagrangian as

$$\frac{\partial L_{\text{eff}}}{\partial a} = \frac{\partial L_{\text{eff}}}{\partial(A^2)} = 0. \tag{20}$$

After straightforward manipulations, Eq. (20) can be cast in the form of expressions for the amplitude and chemical potential in terms of the inverse width:

$$A^2 = \frac{4\sinh(2a)\cdot\sinh^3 a}{(1-g)[\cosh(4a)+2]+3g\cosh(2a)}, \tag{21}$$

$$\mu = 1 - \cosh a + \frac{\sinh^2 a}{\cosh a} \cdot \frac{2g\sinh^2 a + 8\cosh^4 a + 1}{(1-g)[\cosh(4a)+2]+3g\cosh(2a)}. \tag{22}$$
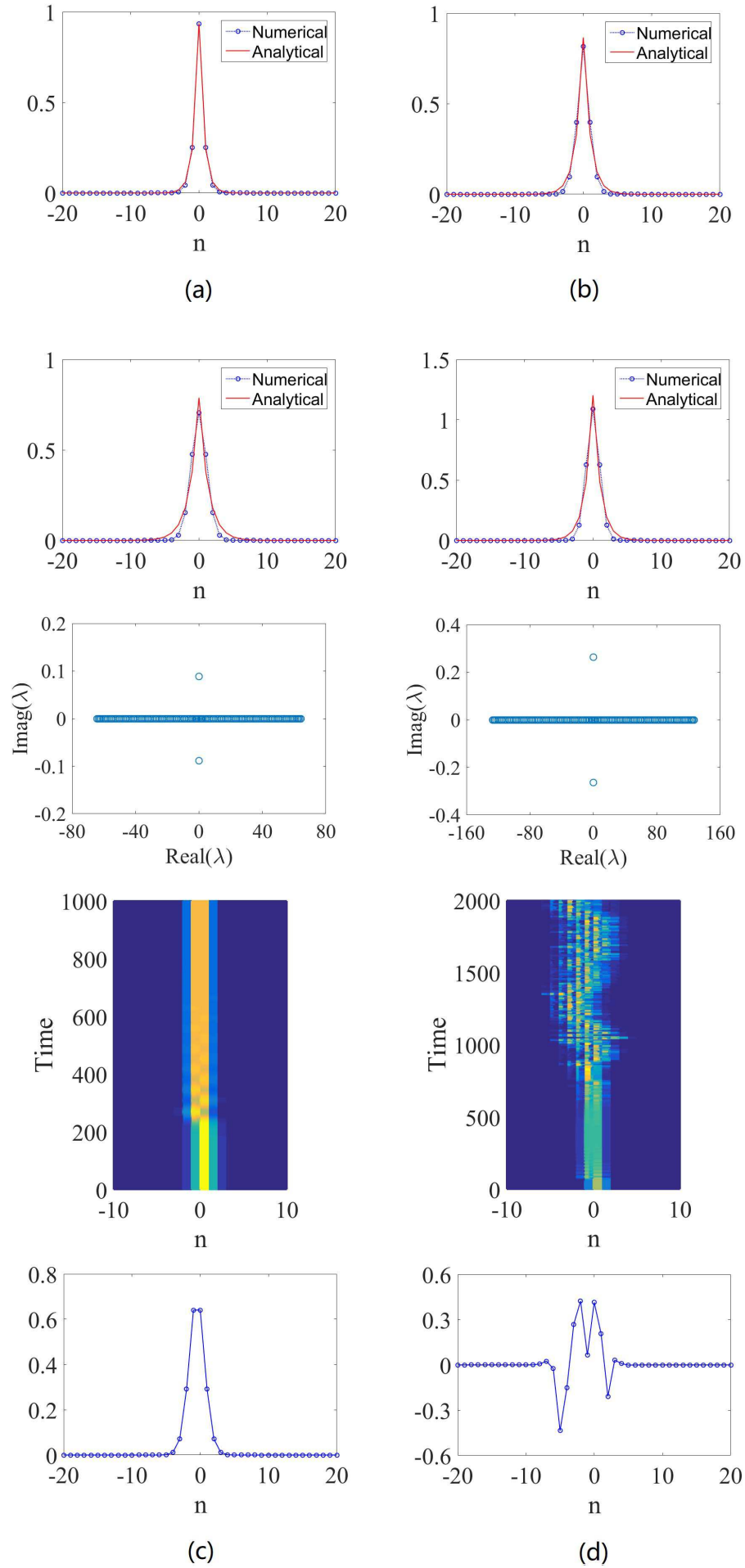
These prediction are compared to numerical findings in the next subsection.

C.   Numerical results

1.   Single-soliton states

Typical examples of fundamental onsite-centered solitons in the zero-detuning system ($\eta = 0$), produced by numerical solution of Eq. (9), along with their analytical counterparts provided by the VA, are demonstrated in Fig. 1. Close agreement between the numerical and variational results is evident. Stability of the discrete solitons was checked both in direct simulations of their perturbed simulations, and through computation of eigenfrequencies, λ, for small perturbations governed by the linearization of Eq. (9), the instability growth rate, if any, being $\text{Im}(\lambda)$. The solitons are completely stable in the cases of $g = -1$ and $g = 0$, i.e., in the cases of the attractive or zero onsite nonlinearity in Eq. (9), independently of the soliton's norm N. In case of $g = +1$, i.e., repulsive onsite interactions, solitons become unstable at sufficiently large N, as shown in Figs. 1(c,d). The bottom panels in (c) and (d) demonstrate the shape of the discrete field observed after long evolution.

We summarize results for the family of such solitons in the form of the dependence of their chemical potential, μ, and width, W, on the norm, N. In the case of $g = 0$, as seen in Fig. 2(b), $\mu(N)$ is a monotonously increasing

(a)

(b)

(c)

(d)

FIG. 1. (Color online) Typical examples of for the results in a one-dimensional conservative system (with random noise
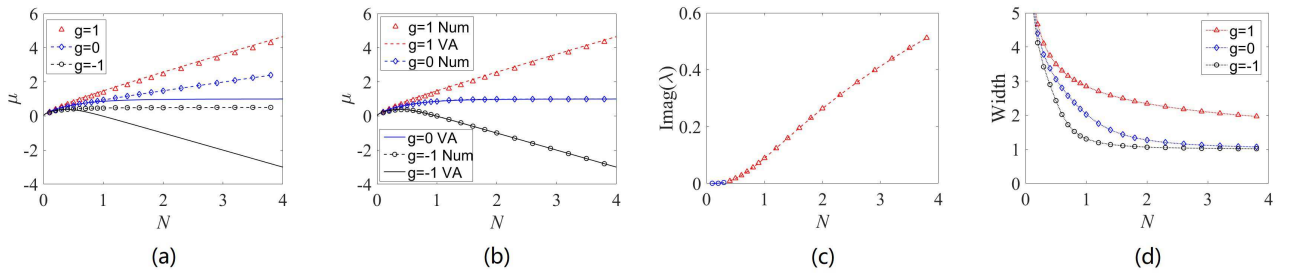
FIG. 2: (Color online) (a) and (b): Dependences $\mu(N)$ for offsite- and onsite-centered discrete solitons at different values of g in the symmetric system ($\eta = 0$). Red triangles, blue diamonds, and black circles present numerical results produced by Eq. (9) for $g = 1$, 0, and -1, respectively. The corresponding variational results are shown in (b) by red dashed, blue, and black solid lines, respectively. (c) Onsite-centered solitons: The instability growth rate of the onsite-centered branch with $g = 1$ versus the total norm, N. The solitons are stable and unstable in regions covered by blue circles and red triangles, respectively, while the branches with $g = -1$ and 0 are completely stable. For the offsite-centered solitons, the situation is opposite: they are completely stable for $g = 1$, and completely unstable for $g = -1$ and 0. (d) The width of the onsite-centered solitons, defined as per Eq. (5), versus N.
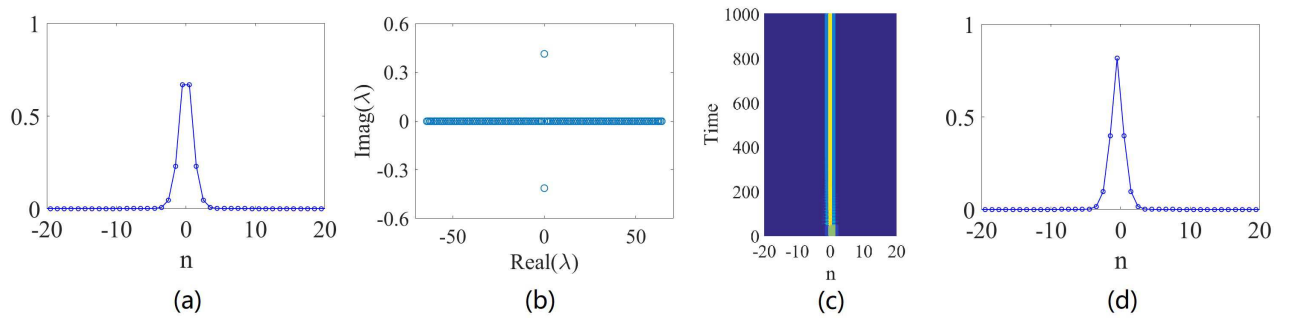

FIG. 3: (Color online) A typical examples of unstable offsite-centered solitons in the symmetric system with $g = 0$ and $N = 1$. Eventually, it transforms into a stable onsite-centered one, which is shown in panel (d).
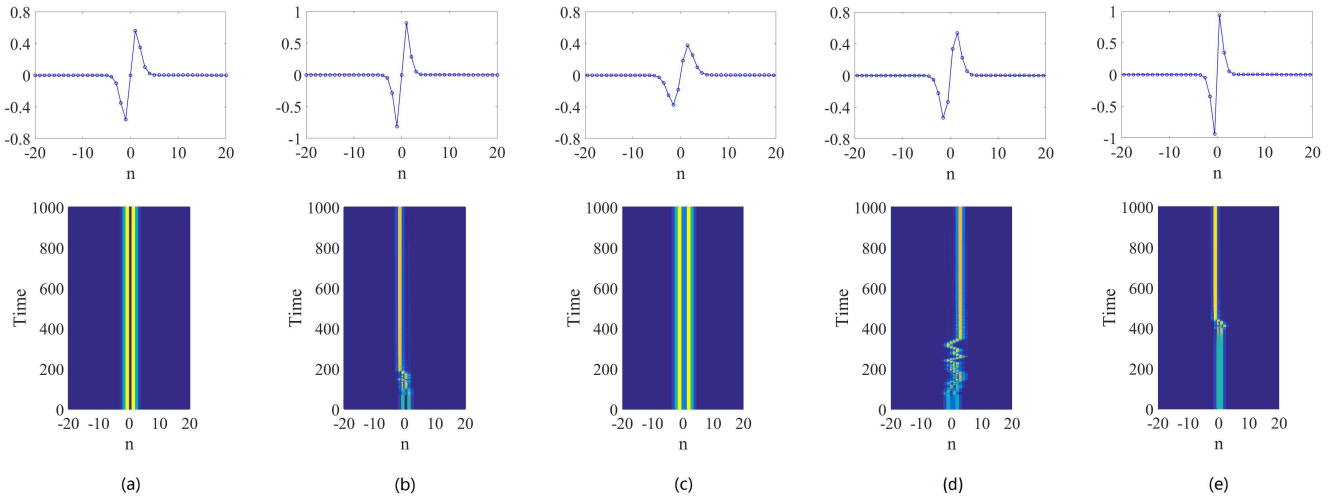

FIG. 4: (Color online) Typical examples of twisted solitons and their evolution in the symmetric system ($\eta = 0$). (a) and (b): Onsite-centered solitons with $N = 0.9$ and $N = 1.5$. (c), (d) and (e): Offsite-centered solitons with $N = 0.5$, $N = 0.9$ and $N = 2$, respectively. The twisted solitons are stable in (a) and (c), and unstable in other cases. In all plots, $g = 0$ (no onsite (contact) nonlinearity).
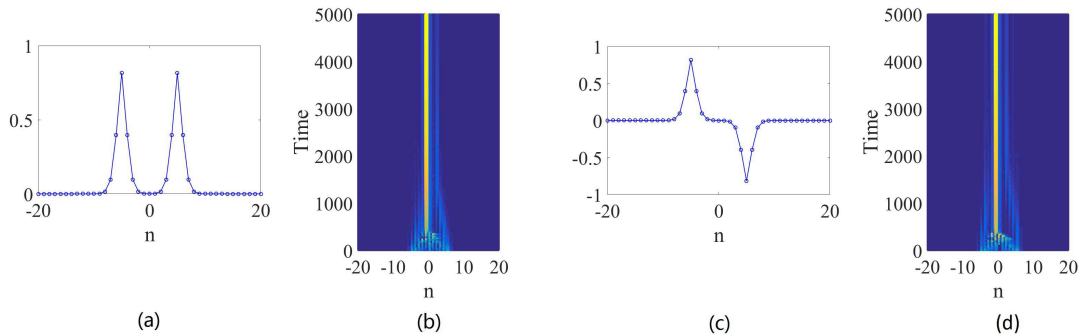
FIG. 5: (Color online) Typical examples of bound states of two fundamental discrete solitons in the symmetric system ($\eta = 0$). (a) and (b): The in-phase bound state and its evolution. (c) and (d): The out-of-phase bound state and its evolution. In all plots, the distance between two peaks is 10.

function with a positive slope, $d\mu/dN > 0$, thus satisfying the *anti-Vakhitov-Kolokolov (VK) criterion*, which is a necessary stability condition for bright solitons supported by repulsive nonlinearities (e.g., gap solitons) [23] (the VK criterion per se, $d\mu/dN < 0$, is necessary for the stability of solitons created by an attractive nonlinearity [24, 25]). On the other hand, in the case of the competition of the nonlocal and contact interactions ($g \neq 0$) the anti-VK and VK criteria may be invalid.

We conclude that the onsite solitons belonging to the branches with $g = 0$ and -1 are stable for all values of the total norm. On the contrary, in the case of $g = 1$ (the self-repulsive onsite nonlinearity), the onsite solitons are stable only at $N \leq 0.4$, being unstable at $N > 0.4$. The analytical predictions produced by the VA, denoted by dashed lines in Fig. 2(b), are in excellent agreement with their numerical counterparts.

The branches of offsite-centered fundamental solitons, which are displayed in Fig. 2(a), feature a totally different behavior. The analysis of their stability readily shows that the branch corresponding to $g = 1$ is *completely stable*, while ones with $g = -1$ and 0 are *completely unstable*. Thus, the system demonstrates *bistability* in the case of $g = 1$ and $N \leq 0.4$, where both offsite- and onsite-centered discrete solitons are stable. In the latter case, the calculation of the respective values of Hamiltonian (14) demonstrates that the solitons of the onsite type realize a smaller value of H, i.e.., they represent the ground state.

Lastly, Fig. 2(d) demonstrates that the discrete solitons shrink under the action of stronger nonlinearity, which corresponds to larger N. Additional simulations demonstrate that unstable offsite-centered solitons tend to spontaneously transform into their stable counterparts of the onsite type, as shown in Fig. 3.

The first excited states in the form of twisted discrete solitons have also been found in the symmetric system, as demonstrated in Fig. 4. These states are stable when norm N is small, e.g., at $N = 0.8$ for the onsite-centered state, and at $N = 0.5$ for the offsite one, see panels (a) and (c), respectively. At larger N, after a sufficiently long evolution the twisted mode eventually evolves into a stable fundamental soliton, which is true for both the onsite and offsite modes, as seen in panels (b), (d) and (e) in Fig. 4. We have identified a critical value of the norm, N_c, above which the twisted states lose their stability: $N_c \simeq 0.96$ and $N_c \simeq 0.59$ for the on- and offsite-centered ones, associated with the twisted patterns containing one or two intermediate sites, respectively (see Fig. 4). Thus, the twisted state of the onsite-centered type is more stable than its offsite counterpart. The number of intermediated sites between two maxima of opposite signs in the twisted state depends on the norm. The larger the norm is, the fewer the number of intermediated sites becomes. In the case of the onsite-centered type, we can find a tightest-shaped twisted mode with only one intermediate site, as shown in Fig. 4(a). Twisted modes of the offsite type contain, as least, two intermediated sites, see Fig. 4(c). For sufficient large N, one can find the tightest offsite-centered twisted state which has no intermediate sites. However, it is found to be unstable, as shown in Fig. 4(e).

2. Bound states of fundamental solitons

We have also constructed bound states of two fundamental solitons of in-phase and out-of-phase types, i.e., with identical and opposite signs of the two constituents, respectively, and with different separations between them. Such bound states, associated with initial separations, are always unstable, finally evolving into single fundamental discrete solitons, as shown in Fig. 5. Naturally, the time for the spontaneous transformation of the in-phase (or out-of-phase) states into fundamental solitons is longer if the initial distance between two peaks is larger.
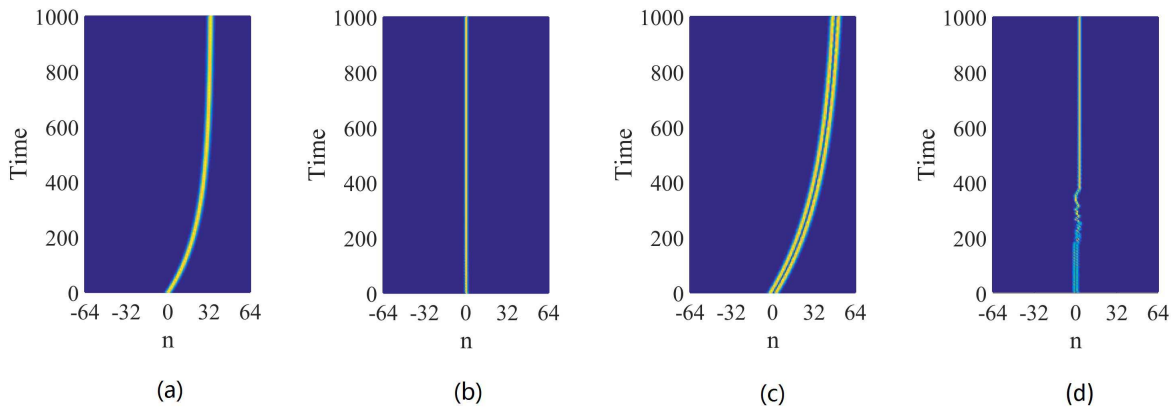
FIG. 6: (Color online) Discrete solitons kicked as per Eq. (23), with $k = 0.05\pi$. (a) and (b): Fundamental solitons with $N = 0.2$ and $N = 1$. (c) and (d): Dipoles with $N = 0.2$ and $N = 1$.
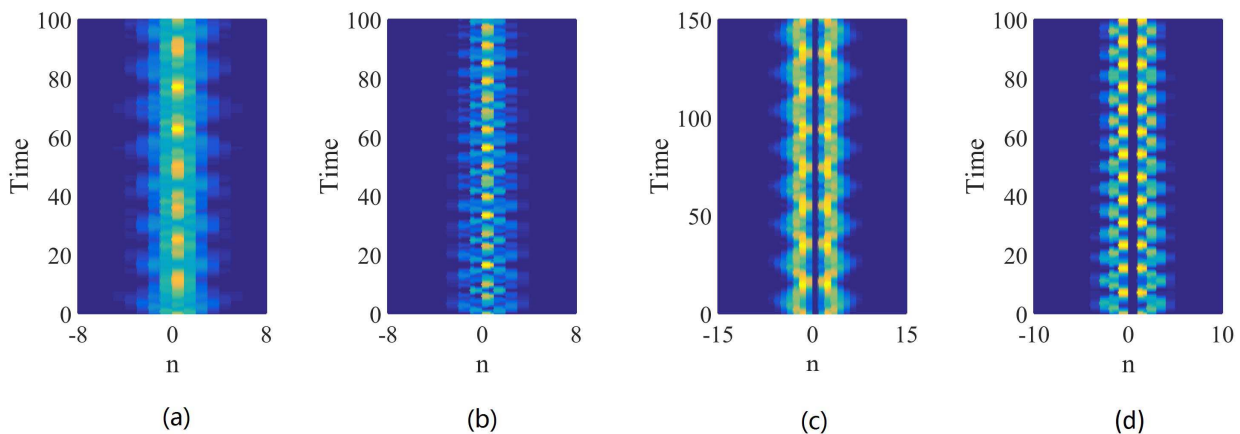

FIG. 7: (Color online) The evolution of discrete solitons to which chirp b is applied. (a) and (b): Fundamental solitons with $N = 0.2$, $b = 0.1\pi$ and $N = 1$, $b = 0.5\pi$. (c) and (d): Twisted solitons with $N = 0.2$, $b = 0.1\pi$ and $N = 1$, $b = 0.5\pi$.

3. Mobility of the discrete solitons

It is well known that, with the exception of integrable systems, such as the Toda [26] and Ablowitz-Ladik [27] lattices, and some other specially designed models [29], rigorous solutions for moving discrete solitons do nor exist. Nevertheless, simulations of the discrete NLSE with the onsite cubic nonlinearity, initiated by a kick, k, applied to a quiescent discrete soliton, u_n, i.e.,

$$U_n(t = 0) = \exp(ikn) u_n, \tag{23}$$

demonstrate its robust mobility: it keeps moving through the lattice indefinitely long, without visible emission of radiation waves ("phonons") or loss of the velocity [31]-[35].

To address the possible mobility of the solitons in the present system, we have performed simulations of Eq. (1) with initial conditions (23). At small N, the fundamental soliton sets in motion, but eventually it comes to a halt, as shown in Fig. 6(a). When N is sufficiently large, the kicked soliton does not feature even transient mobility, remaining quiescent, as shown in Fig. 6(b). Thus, the present system is drastically different in terms of the soliton's mobility from the discrete NLSE with the local cubic term.

The mobility of twisted discrete solitons was studied too. It was found that their dynamics is similar to that of the fundamental ones when N is small (e.g., for $N = 0.2$), i.e., the kicked twisted state features transient mobility. However, when N increases to 1, the kick destroys the twisted state, in contrast to the situation for the robust fundamental solitons.

In addition, it is possible to simulate effects of real *chirp b* applied to the fundamental and twisted discrete solitons, by solving Eq. (1) with initial condition

$$U_n(t=0) = \exp\left(ib|n|\right) u_n. \tag{24}$$

The results displayed in Fig. 7 demonstrate excitation of robust internal modes in both the fundamental and twisted solitons as the reaction to the application of the chirp.

IV. THE ASYMMETRIC (DETUNED) SYSTEM

A. An analytical approximation for strong asymmetry

To address the general form of Eq. (1), which includes detuning η, it is relevant to start from the limit case of large η (strong detuning), when the approximation which was developed, for the continuum systems, in works [5] and [36] suggests that this case may be effectively reduced to a single equation, by eliminating the small higher-energy component in favor of the large lower-energy one. To this end, the underlying wave functions are redefined as

$$(\Psi_n, \Phi_n) \equiv e^{i\eta t}\left(\tilde{\Psi}_n(t), \tilde{\Phi}_n(t)\right). \tag{25}$$

Substituting this in Eq. (1) for Ψ_n leads, in the first approximation, to relation

$$\tilde{\Psi}_n = (H_0/2\eta)\,\tilde{\Phi}_n. \tag{26}$$

Next, the substitution of this relation in the equation for Φ_n produces an equation which, up to a shift of the chemical potential and different notation for the coefficient, is tantamount to Eq. (7):

$$i\frac{\partial\tilde{\Phi}_{nn}}{\partial t} = -\frac{1}{2}\left(\tilde{\Phi}_{n+1} - 2\tilde{\Phi}_n + \tilde{\Phi}_{n-1}\right) - \frac{H_0^2}{2\eta}\tilde{\Phi}_n + \frac{\gamma H_0^2}{4\eta^2}\tilde{\Phi}_n\sum_m|m-n||\tilde{\Phi}_m|^2 + \Gamma\left|\tilde{\Phi}_n\right|^2\tilde{\Phi}\bigg|_n. \tag{27}$$

Thus, the limit case of strong asymmetry between the two components leads to essentially the same single GPE as in the case of the fully symmetric system.

B. Numerical results

In the presence of finite detuning, a typical example of a stable two-component discrete soliton with components ψ_n and ϕ_n (see Eq. (2) along with simulations of its evolution, initiated by the addition of small random perturbations, is displayed in Fig. 8.

In the case of large detuning, the full numerical solution for a stable fundamental discrete soliton is compared to the approximation, based on Eqs. (26) and (27), in Fig. 9. It is seen that the approximation is accurate for the strongly asymmetric solitons.

The width of the fundamental discrete solitons is plotted, as a function of the background magnetic field, the strength of the Zeeman splitting, and the strength of the long-range interaction, in Fig. 10. It is seen that the increase of the background field and strength of the long-range interaction leads to shrinkage of the solitons. On the contrary, stronger Zeeman splitting makes the solitons wider. Note that the width of the fundamental discrete solitons diverges in the limit of $H_0 \to 0$, while, in the case of $\eta = 0$, the solution does not depend on H_0, as seen in panel (b).

Lastly, to consider the distribution of the total norm (which is now scaled to be $N = 1$) between the two components (ψ, ϕ) of the asymmetric discrete solitons, a typical example of the dependence of the component norms on the background magnetic field is shown in Fig. 11(a). One can see that the difference between the lower- and higher-energy components decreases as H_0 increases, because the effect of the Zeeman splitting is suppressed by the background field. The dependence of the norms on η is shown in panel (b), which naturally implies that the Zeeman splitting enhances the asymmetry.

V. CONCLUSION

We have introduced a two-component discrete system which models the pseudospinor BEC, whose components are coupled by the microwave field, while the condensate is made effectively discrete by a deep optical-lattice potential.
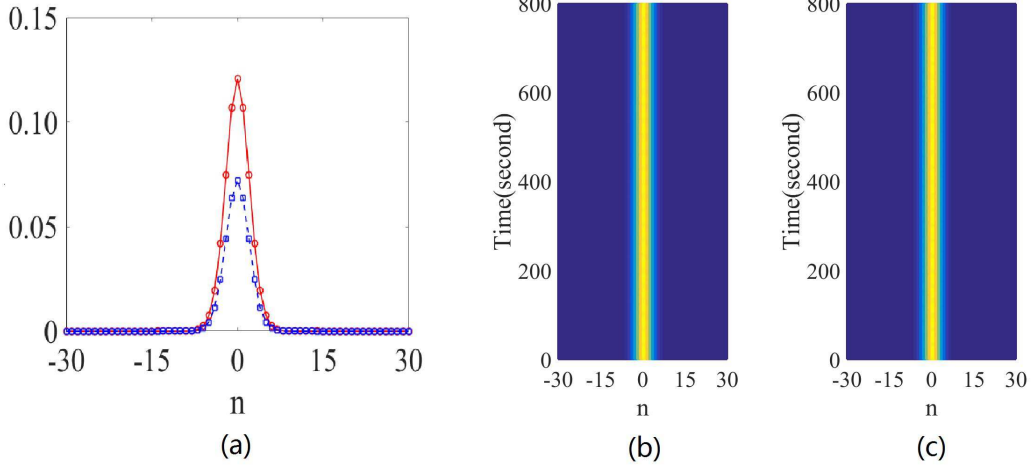
FIG. 8: (Color online) (a) A typical example of the two components ϕ and ψ of the fundamental discrete soliton (red circles and blue squares, respectively) in the asymmetric (mismatched) system. (b) and (c): The perturbed evolution of the $|\Psi|$ and $|\Phi|$ components, corroborating stability of this soliton. The parameters are $N = 1$, $\eta = 0.5$, $H_0 = 2$, and $\gamma = 0.1$.
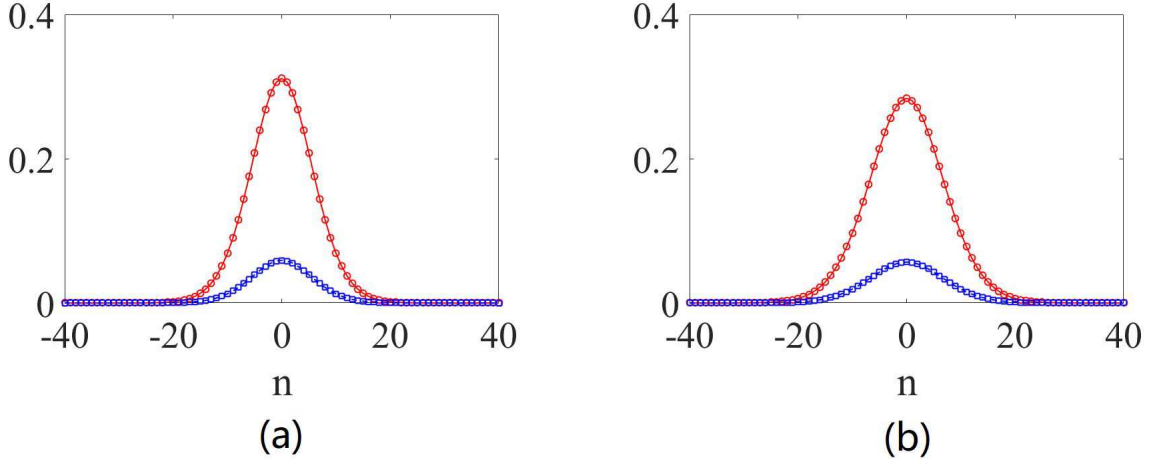

FIG. 9: (Color online) (a) Typical examples of components ϕ_n and ψ_n (blue circles and black squares, respectively) of the fundamental discrete soliton in the strongly asymmetric system, as produced by Eq. (1). Red diamonds and blue stars depict the corresponding approximation produced by Eqs. (26) and (27). The parameters are $\eta = 10$, $H_0 = 4$, $\gamma = 0.1$, and $N = 1$.

The elimination of the field by means of the Green's function of the one-dimensional Poisson equation gives rise to a long-range self-trapping interaction between lattice sites, which can be combined with the usual onsite cubic nonlinearity of either sign. The numerical solution shows that onsite-centered fundamental solitons are stable in the case of zero and attractive onsite interactions, while offsite-centered fundamental solitons are unstable. The situation is opposite in the case of the repulsive onsite nonlinearity: solitons of the offsite type are stable, while onsite-centered ones are stable only at sufficiently small values of the norm, at which the system features the bistability of the onsite and offsite-centered fundamental solitons. The variational approximation very accurately predicts the shape of the onsite-centered solitons. The first excited states, in the form of twisted solitons, are stable at small values of the norm, while at large norms they are subject to an instability which transforms them into fundamental solitons. Bound states of two fundamental solitons of both in-phase and out-of-phase types are unstable, evolving into a single fundamental-like soliton. Another specific feature of the system is that it does not admit mobility of the discrete solitons.

In the asymmetric version of the system, the background magnetic field tends to compress the solitons and suppress the asymmetry between the lower- and higher- components, while the Zeeman splitting plays an opposite role. In the limit case of strong asymmetry, the two-component system can be approximately reduced to a single discrete GPE
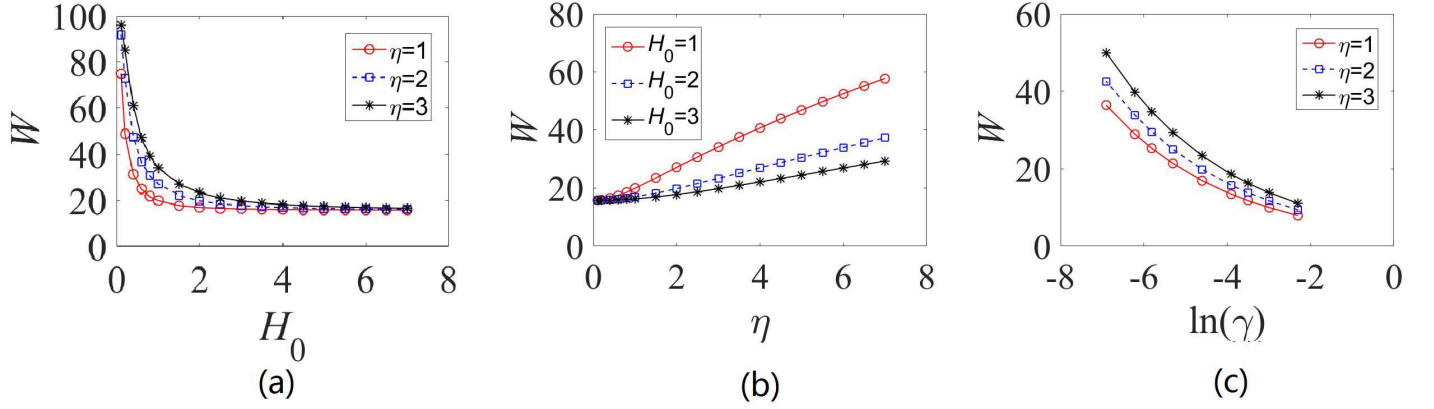
FIG. 10: (Color online) (a) The width of fundamental discrete solitons versus background magnetic field H_0 for a fixed value of the strength of the long-range interaction, $\gamma = 0.01$, and different values of the Zeeman-splitting coefficient, η. (b) The width versus η for $\gamma = 0.01$ and different values of H_0. (c) The width versus $\ln(\gamma)$ for $H_0 = 2.0$ and different values of η. In all plots, $N = 1$.
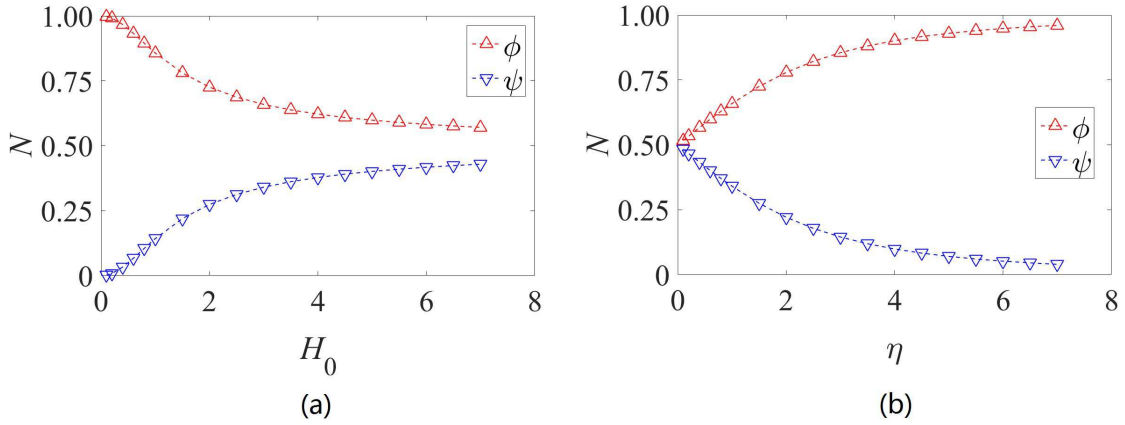

FIG. 11: (Color online) (a) A typical example of norms of the ψ and ϕ components as functions of H_0 for $\eta = 1$. (b) The dependence of the norms on η for $H_0 = 3$. In all plots, $N = 1$ and $\gamma = 0.01$.

(Gross-Pitaevskii equation), which is corroborated by numerical results.

A challenging direction for further work is to introduce a two-dimensional version of the system and construct two-dimensional discrete solitons in it, including discrete vortices.

VI.   ACKNOWLEDGEMENTS

[1] Brazhnyi V A and Konotop V V 2004 Mod. Phys. Lett. B 18 627-651.
[2] Morsch O and Oberthaler M 2006 Rev. Mod. Phys. 78 179-215.
[3] Li K, Deng L, Hagley E W, Payne M G and Zhan M S 2008 Phys. Rev. Lett. 101 250401.
[4] Zhu J, Dong G J, Shneider M N and Zhang W P 2011 Phys. Rev. Lett. 106 210403.
[5] Dong G, Zhu J, Zhang W and Malomed B A 2013 Phys. Rev. Lett. 110 250401.

[6] Qin J, Dong G and Malomed B A 2015 Phys. Rev. Lett. 115 023901.
[7] Qin J, Dong G and Malomed B A 2016 Phys. Rev. A 94 053611.
[8] Trombettoni A and Smerzi A 2001 Phys. Rev. Lett. 86 2353.
[9] Abdullaev F Kh, Baizakov B B, Darmanyan S A, Konotop V V and Salerno M 2001 Phys. Rev. A 64 043606.
[10] Alfimov G L, Kevrekidis P G, Konotop V V and Salerno M 2002 Phys. Rev. E 66 046608.
[11] Carretero-González R and Promislow K 2002 Phys. Rev. A 66 033610.
[12] Efremidis N K and Christodoulides D N 2003 Phys. Rev. A 67 063608; Maluckov A, Hadžievski L, Malomed B A and Salasnich L 2008 Phys. Rev. A 78 013616.
[13] Gligorić G, Maluckov A Hadžievski L and Malomed B A 2008 Phys. Rev. A 78 063615.
[14] Maluckov A, Gligorić G, Hadžievski Lj, Malomed B A and Pfau T 2012 Phys. Rev. Lett. 108 140402.
[15] Lederer F, Stegeman G I, Christodoulides D N, Assanto G, Segev M and Silberberg Y 2008 Phys. Rep. 463 1-126.
[16] Kevrekidis P G 2009 *The Discrete Nonlinear Schrödinger Equation: Mathematical Analysis, Numerical Computations, and Physical Perspectives* (Springer: Berlin and Heidelberg, 2009).
[17] Gaididei Y B, Mingaleev S F, Christiansen P L and Rasmussen K O 1997 Phys. Rev. E 55 6141-6150.
[18] Darmanyan S, Kobyakov A and Lederer F 1998 Zh. Eksp. Teor. Fiz. 113 1253-1260[English translation: 1998 J. Exp. Theor. Phys. 86 682-686].
[19] Kevrekidis P G, Bishop A R and Rasmussen K O 2001 Phys. Rev. E 63 036603.
[20] Juzeliūnas G, Ruseckas J and Dalibard J 2010 Phys. Rev. A 81 053403.
[21] Gligorić G, Maluckov A, Hadzievski L and Malomed B A 2013 Phys. Rev. E 88 032905.
[22] Barbiero L, Malomed B A and Salasnich L 2014 Phys. Rev. A 90 063611.
[23] Sakaguchi H and Malomed B A 2010 Phys. Rev. A 81 013624.
[24] Vakhitov M and Kolokolov A 1973 Radiophys. Quantum Electron. 16 783.
[25] Bergé L 1998 Phys. Rep. 303 259.
[26] Toda M 1967 J. Phys. Soc. Jpn. 22 431-436.
[27] Ablowitz M J and Ladik J F 1976 J. Math. Phys. 17 1011-1018.
[28] Friesecke G and Wattis J A D 1994 Comm. Math. Phys. 161 391-418.
[29] Oxtoby O F, Pelinovsky D E and Barashenkov I V 2006 Nonlinearity 19 217-235.
[30] Barashenkov I V and van Heerden T C 2008 Phys. Rev. E 77 036601.
[31] Duncan D B, Eilbeck J C, Feddersen H and Wattis J A D 1993 Physica D 68 1.
[32] Flach S and Kladko K 1999 Physica D 127 61.
[33] Flach S, Zolotaryuk Y and Kladko K 1999 Phys. Rev. E 59 6105.
[34] Ablowitz M J, Musslimani Z H and Biondini G 2002 Phys. Rev. E 65 026602.
[35] Papacharalampous I E, Kevrekidis P G, Malomed B A and Frantzeskakis D J 2003 Phys. Rev. E 68 046604.
[36] Sakaguchi H, Sherman E Ya and Malomed B A 2016 Rev. E 94 032202.
[37] Marin J L and Aubry S 1996 Nonlinearity 9 1501-1528.
[38] Pitaevskii L P and Stringari A 2003 *Bose-Einstein Condensation* (Clarendon Press, Oxford, 2003).
[39] Malomed B A and Weinstein M I 1996 Phys. Lett. A 220 91-96.
[40] Kaup D J 2005 Math. Comp. Simul. 69 322-333.
[41] Malomed B A, Kaup D J and Van Gorder R A 2012 Phys. Rev. E 85 026604.